Hindawi
Science and Technology of Nuclear Installations
Volume 2021, Article ID 9997867, 13 pages
https://doi.org/10.1155/2021/9997867

Research Article

Study on the Sensitivity and Uncertainty of Nuclear Data to the Sodium-Cooled Linear Breed-and-Burn Fast Reactor Using SCALE6.2 Code

Thanh Mai Vu [1] **and Donny Hartanto** [2,3]

[1] *VNU University of Science, Vietnam National University, Hanoi 334 Nguyen Trai, Thanh Xuan, Hanoi 120-034, Vietnam*
[2] *Department of Mechanical and Nuclear Engineering, University of Sharjah, P.O. BOX 27272, Sharjah, UAE*
[3] *Nuclear Energy System Simulation and Safety Research Group, Research Institute for Sciences and Engineering, University of Sharjah, P.O. BOX 27272, Sharjah, UAE*

Correspondence should be addressed to Thanh Mai Vu; mai_vu@hus.edu.vn

Received 12 March 2021; Revised 20 June 2021; Accepted 30 June 2021; Published 13 July 2021

Academic Editor: Guglielmo Lomonaco

Previously, the neutronics design of a small and compact linear breed-and-burn fast reactor (B&BR) was completed. The reactor produces 400 MWth power, and it can operate with excess reactivity of less than 1$ for more than 50 years without refuelling. As the blanket fuel, the spent nuclear fuel (SNF) from existing light water reactors (LWRs) is used to reduce the burden from the problematic long-lived isotopes in SNF. However, by loading massive nuclides at the initial core, the impact of nuclear data uncertainty on the reactivity calculation results of SNF-fuelled B&BR at the beginning of life (BOL) is expected to be significant because these nuclides have different credentials in evaluated nuclear data libraries. In this study, the impact of nuclear library uncertainty from ENDF/B-VII.0 and ENDF/B-VII.1 on reactivity calculation of B&BR is evaluated using the continuous-energy TSUNAMI-3D module in the SCALE6.2 code package. The uncertainty of reactivity calculation results of B&BR caused by the inaccuracy of two libraries is significant (more than 2000 pcm), mainly from the uncertainty of ^{235,238}U and ^{56}Fe cross section. The energy-dependent sensitivity profiles show that they are significant at the fast energy range. The uncertainty of coolant void reactivity (CVR) is about 18%, and that of fuel temperature coefficient (FTC) is about 15% of the reactivity effect. The top five contributions for CVR accounted for elastic scattering of ^{238}U, capture of ^{235,238}U, and elastic scattering of ^{23}Na and ^{56}Fe. Meanwhile, the top contributors for FTC were accounted for elastic scattering of ^{238}U and ^{56}Fe, capture of ^{235}U, and elastic scattering of ^{94}Zr and ^{57}Fe. It is highly recommended to improve the accuracy of those isotopes' cross sections at the high energy range to provide a more reliable reactivity calculation for the fast system.

1. Introduction

The breed-and-burn fast reactor (B&BR) is an attractive design because it offers a higher fuel utilization than the traditional fast reactor (>20% burnup). It is possible because B&BR can breed its fuel and use the bred fuel to achieve an extremely long lifetime. Therefore, the B&BR is usually designed to have a thick blanket fuel region loaded with natural uranium, depleted uranium, or spent nuclear fuel. The blanket fuel region can be placed as an axial or radial blanket. Next to the blanket fuel region, the initial core region is located, and it is loaded with low-enriched uranium fuel. The initial core region starts the criticality and supplies neutrons to the blanket region. The active core will gradually produce fissile isotopes from the fertile isotopes in the blanket region, and these bred fissile isotopes will be used to maintain the criticality.

Recently, a small and compact linear B&BR has been designed [1–5]. It is considered a linear type because the blanket region is an axial blanket, and the breed-and-burn wave travels linearly from the initial core to the blanket region. The breed-and-burn wave discontinues when it

reaches the end of the blanket region. Therefore, it can be concluded that, in the linear B&BR, the core lifetime depends on the length of the blanket region. The recently designed reactor is also attractive. Besides being safer by producing lower power, it uses spent nuclear fuel (SNF) from the existing light water reactors (LWRs) as its blanket fuel to reduce the environmental burden from the problematic long-lived isotopes in the SNF. A more detailed core design and major parameters are explained in the subsequent section.

For the blanket fuel, the SNF is recycled using a simplified melt refining process adopted for EBR-II from 1964 to 1969. In the process, the gaseous and volatile isotopes are assumed completely removed, while the rare earth and reactive isotopes are removed by 95%, and the noble metals, uranium, and transuranium are assumed to be recovered by 100%. The spent fuel of PWR with a history of 50 GWd/MTHM and ten-yeas cooling is considered. It is expected that the blanket fuel consists of almost all isotopes available in the nuclear data library.

Previously, the neutronics simulations of this core were conducted using the McCARD Monte Carlo code [5]. In the Monte Carlo (MC) code calculation, by using a sufficient number of histories, the statistical deviation of the simulation results can be reduced to be adequately small. Thus, the uncertainty of the evaluated nuclear data libraries used in the calculation is expected to be the main contributor to the overall uncertainty and affects the reliability of the calculation results. In recent investigations about the impact of nuclear data on the calculated k_{eff} of the fast system, the results show a significant uncertainty originated from the errors of the cross section libraries [6–8]. However, the sensitivity and uncertainty (S/U) analyses done for fast systems are still limited and do not cover a wide range of isotopes. In this work, by loading massive nuclides as the blanket core with different credentials in the evaluated nuclear libraries, the impact of nuclear data uncertainty on the reactivity calculation results of SNF-fuelled B&BR is expected to be significant. Thus, the sensitivity and uncertainty analyses on linear B&BR at BOL for two ENDF nuclear library versions (ENDF/B-VII.0 [9] and ENDF/B-VII.1 [10]) were conducted using SCALE6.2 and presented and discussed in this study for the first time. The findings from the analyses will also provide feedback on how much the accuracy of the later version of the nuclear data library has been improved compared to the older ENDF/B-VII.0 library. The multigroup-covariance matrices of the two nuclear data library versions are available in SCALE6.2 [11]. The continuous-energy TSUNAMI-3D (Tools for Sensitivity and Uncertainty Analysis Methodology Implementation in Three Dimensions) and TSAR (Tool for Sensitivity Analysis of Reactivity Responses) modules within SCALE6.2 were used to complete the analysis.

This paper is organized as follows: Section 2 discusses the design of the small and compact linear B&BR. The methodology used to quantify the sensitivity and uncertainty is explained in Section 3, followed by the results and discussion in Section 4. Finally, the conclusion and future recommendations are presented in Section 5.

2. B&BR Design

The B&BR is designed to produce a 400 MWth power, and the core comprises 78 fuel assemblies. There are seven control element assemblies in the core, and they are divided into four primary and three secondary control assembly groups. A relatively thick PbO reflector (3 rings or 126 reflector assemblies) improves the neutron reflection performance [12]. A ring of shield assemblies surrounds the core. The radial core configuration is shown in Figure 1.

Meanwhile, there are several fuel zones in the axial direction. The initial LEU driver core is a concave-shaped core fuelled with LEU–10Zr and LEU–7Zr. The uranium enrichment is 12.32% in the driver core region. Meanwhile, in the blanket region, it is fuelled with SNF–8Zr and SNF–6Zr. The major vector composition of the spent fuel (wt. > 0.1%) is summarized in Table 1.

The fuel, HT9 structure, and sodium coolant volume fractions in each fuel assembly are 63.34%, 14.01%, and 22.65%.

The total core height is 180 cm, and the axial configuration can be seen in Figure 2. The coolant inlet and outlet temperatures are assumed to be 360°C and 510°C, similar to the coolant temperature of a typical sodium-cooled fast reactor. The average sodium coolant speed is calculated to be about 2.94 m/s. A more detailed description of the core can be found in several references [4, 5].

3. Methodology and Calculation Tool

In the S/U analysis, SCALE6.2 code [11, 13] was used. In SCALE6.2, the (S/U) analysis can be performed by calling three modules: KENO-VI to perform the neutronics calculations and TSUNAMI-3D and TSAR to perform the sensitivity and uncertainty calculation. The KENO-VI produces a best-estimate eigenvalue with one standard deviation computed as the minimum variance of eigenvalue based on active generations run, representing the MC method statistical uncertainty. In the TSUNAMI-3D module, the general perturbation theory (GPT) performs forward and adjoint KENO-VI calculations to compute k_{eff} and execute SAMS to generate the required sensitivity coefficients to predict the relative changes in a systems' calculated k_{eff} value. The sensitivity analysis obtained by the MC method has overcome the difficulty of geometry modelling in a deterministic method such as the SAGEP code [14] which would also cause the uncertainty of the uncertainty analysis results. In this study, 44-group and the 56-group structure sensitivity coefficients were generated for ENDF/B-VII.0 and ENDF/B-VII.1, respectively. In SAMS, both explicit sensitivity (the sensitivity of the system responses to the problem-dependent resonance self-shielded multigroup cross section data used in the analysis) and implicit sensitivity (the sensitivity of the resonance self-shielded multigroup cross section data to the data input to the resonance self-shielding calculation) were calculated. Summing the implicit and explicit contributions from a particular cross section data component produces the complete sensitivity coefficient:

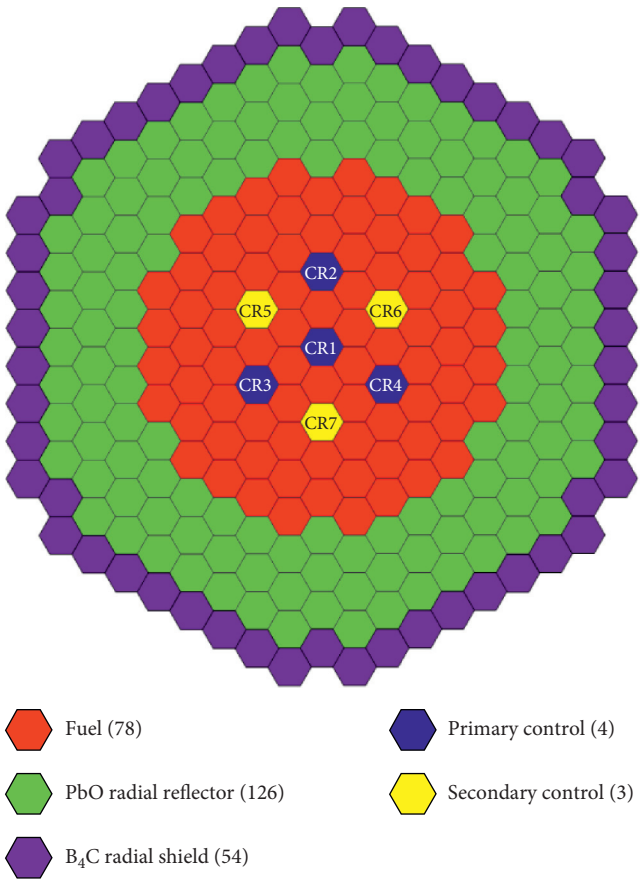

Figure 1: Radial sectional view of B&BR.

Table 1: Major SNF vectors of blanket fuel in B&BR.

Isotope	wt.%
Sr	$1.16E-01$
Zr	$5.69E-01$
Mo	$5.23E-01$
Tc	$1.19E-01$
Ru	$3.53E-01$
Pd	$2.24E-01$
Ba	$2.85E-01$
^{234}U	$2.32E-02$
^{235}U	$8.92E-01$
^{236}U	$6.40E-01$
^{238}U	$9.47E+01$
^{237}Np	$7.80E-02$
^{238}Pu	$3.30E-02$
^{239}Pu	$6.30E-01$
^{240}Pu	$2.89E-01$
^{241}Pu	$1.10E-01$

$$\left(S_{k,\Sigma^i_{x,g}}\right)_{\text{complete}} = \left(S_{k,\Sigma^i_{x,g}}\right)_{\text{explicit}} + \left(S_{k,\Sigma^i_{x,g}}\right)_{\text{implicit}}, \quad (1)$$

where $S_{k,\Sigma^i_{x,g}}$ is the groupwise sensitivity of k_{eff} to the cross section of nuclide i in reaction x.

After achieving the sensitivity coefficients, SAMS reads the covariance data from a standard COVERX data file and

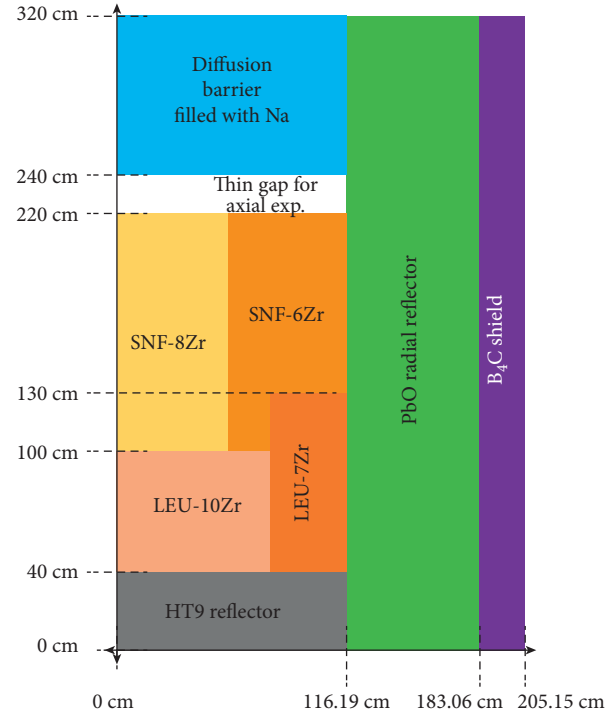

Figure 2: Axial sectional view of B&BR.

the variance for the system k_{eff} due to the changes in the neutron cross section data is produced as follows:

$$U = \sqrt{\sigma_k^2} = \sqrt{S_k^T \cdot C_{\Sigma\Sigma} \cdot S_k}, \quad (2)$$

where S_k is the sensitivity coefficient, in this investigation, in 44-group/56-group energy structure and T indicates transpose; the element of S_k is

$$\left(S_{k,\Sigma^i_{x,g}}\right) = \frac{\Sigma^i_{x,g}}{k}\frac{\partial k}{\partial \Sigma^i_{x,g}}, \quad (3)$$

and $C_{\Sigma\Sigma}$ is 44-group/56-group covariance data from a standard COVERX data file, and the element of $\mathbf{C}_{\Sigma\Sigma}$ is

$$\left(C_{\Sigma^i_{x,g}\Sigma^j_{y,g'}}\right) = \frac{\text{COV}\left(\Sigma^i_{x,g}\Sigma^j_{y,g'}\right)}{\Sigma^i_{x,g}\Sigma^j_{y,g'}}, \quad (4)$$

where $\Sigma^i_{x,g}$ and $\Sigma^j_{y,g'}$ are the cross section with i and j varied over all isotopes, x and y varied over all reactions for each isotope, and g and g' varied over all energy groups.

In this work, TSUNAMI-3D was employed to evaluate the uncertainty caused by the error of evaluated cross section libraries, ENDF/B-VII.0 and ENDF/B-VII.1, and in the case when the CE library is used in a TSUNAMI calculation, only the forward KENO-VI calculation is performed. A general flow diagram of a CE calculation with TSUNAMI is shown in Figure 3.

For calculating the uncertainty caused by other changes rather than the errors of cross section data such as temperature or void fraction, the TSAR module is called. TSAR reads the sensitivity data files (.sdf file) produced by

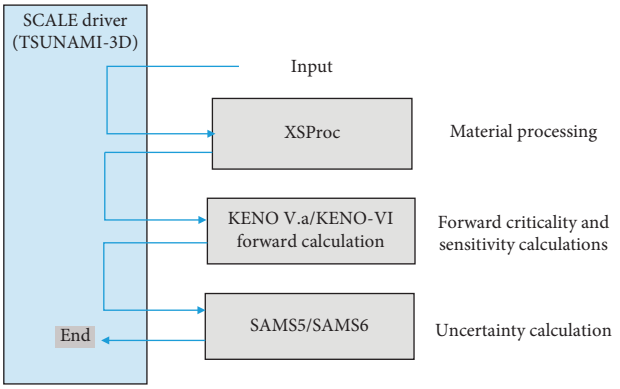

Figure 3: General flow diagram of CE TSUNAMI-3D.

Table 2: Major sensitivities of k_{eff} (positive direction).

Isotopes	Nuclear data	Sensitivity for ENDF/B-VII.0	Sensitivity for ENDF/B-VII.1
^{235}U	ν, ν	$8.07E-01$	$8.06E-01$
^{235}U	σ_f, σ_f	$5.28E-01$	$5.28E-01$
^{238}U	ν, ν	$1.85E-01$	$1.86E-01$
^{238}U	σ_f, σ_f	$1.12E-01$	$1.12E-01$
^{238}U	σ_{el}, σ_{el}	$2.17E-02$	$2.21E-02$
^{56}Fe	σ_{el}, σ_{el}	$1.06E-02$	$1.11E-02$
^{23}Na	σ_{el}, σ_{el}	$8.42E-03$	$8.76E-03$
^{208}Pb	σ_{el}, σ_{el}	$7.87E-03$	$7.73E-03$
^{239}Pu	ν, ν	$5.85E-03$	$5.88E-03$

Table 3: Major sensitivities of k_{eff} (negative direction).

Isotopes	Nuclear data	Sensitivity for ENDF/B-VII.0	Sensitivity for ENDF/B-VII.1
^{238}U	σ_c, σ_c	$-2.49E-01$	$-2.48E-01$
^{238}U	σ_{ine}, σ_{ine}	$-7.08E-02$	$-7.11E-02$
^{235}U	σ_c, σ_c	$-6.45E-02$	$-6.42E-02$
^{56}Fe	σ_c, σ_c	$-1.10E-02$	$-1.09E-02$
^{56}Fe	σ_{ine}, σ_{ine}	$-1.09E-02$	$-1.11E-02$
^{235}U	σ_{ine}, σ_{ine}	$-7.48E-03$	$-7.48E-03$

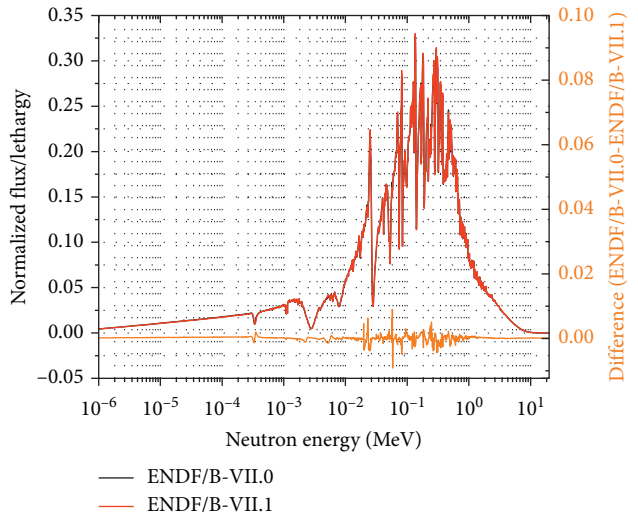

Figure 4: The neutron spectra of the B&BR.

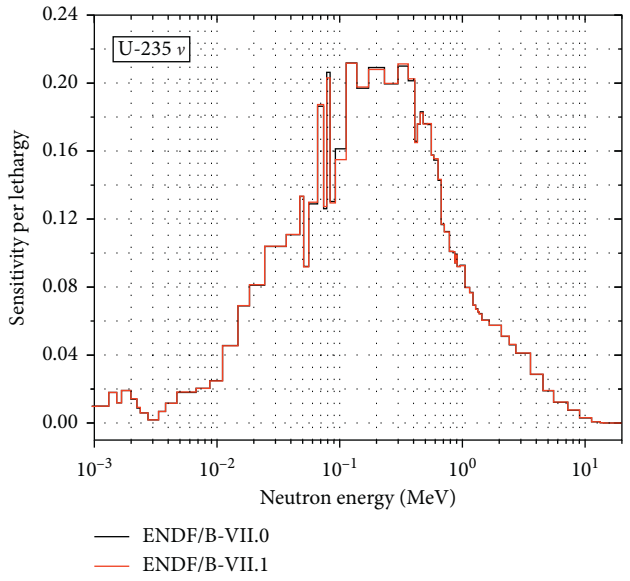

Figure 5: Energy-dependent sensitivities of k_{eff} to ^{235}U total ν cross section.

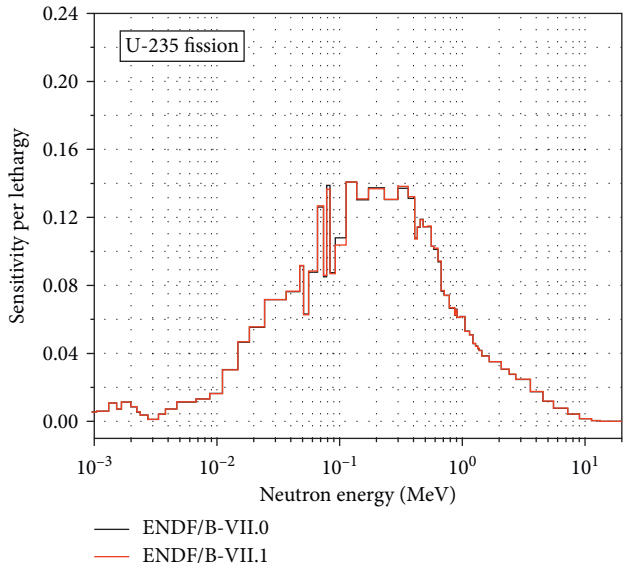

Figure 6: Energy-dependent sensitivities of k_{eff} to ^{235}U fission cross section.

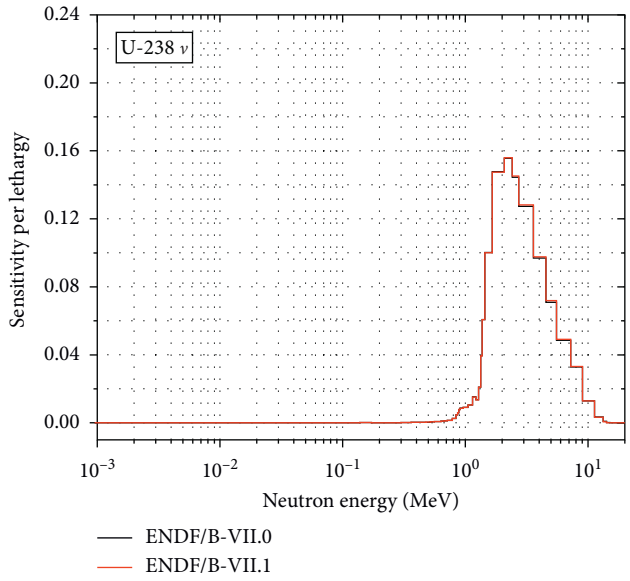

Figure 7: Energy-dependent sensitivities of k_{eff} to ^{238}U total ν cross section.

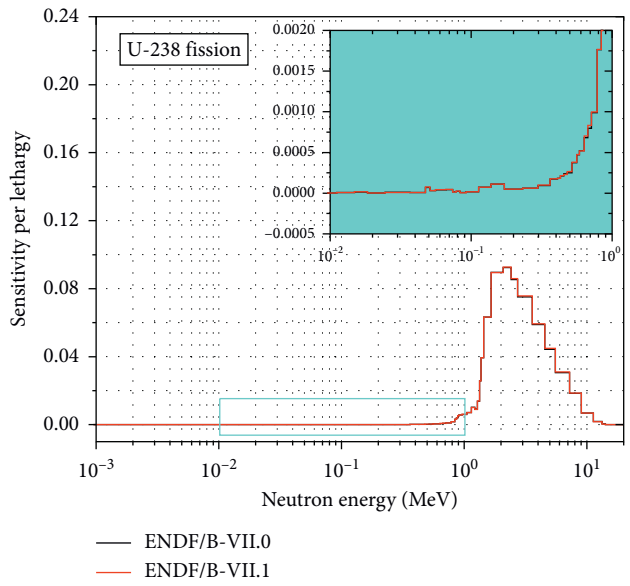

Figure 8: Energy-dependent sensitivities of k_{eff} to ^{238}U fission cross section.

TSUNAMI k_{eff} calculations and uses them to compute relative or absolute sensitivities of an eigenvalue-difference response. Then, it combines the calculated reactivity sensitivity coefficients with input nuclear data covariance matrices included in SCALE to determine the uncertainty of the reactivity response. The SCALE covariance data libraries used in this work were the 44-group data based on ENDF/B-VII.0 and the 56-group data based on ENDF/B-VII.1. In SCALE calculations, 100,000 histories, 3000 active cycles, and 1000 inactive cycles were used to obtain the standard deviation less than 4×10^{-5}. The computing time for each case was about 14 hours using 72 cores.

4. Results and Discussion

4.1. Sensitivity Analysis. The sensitivities of k_{eff} obtained for ENDF/B-VII.0 and ENDF/B-VII.1 nuclear data libraries on B&BR were classified into negative and positive values and are presented in Tables 2 and 3. Those with an absolute value larger than 0.005 and impact of the uncertainty of reactivity calculation results are further discussed. For positive sensitivity coefficient, the results reveal that the total ν, fission cross section, and elastic scattering of nuclides in the fuel, coolant, cladding, and reflector have significant sensitivity coefficients of k_{eff}, especially at the high energy range, and

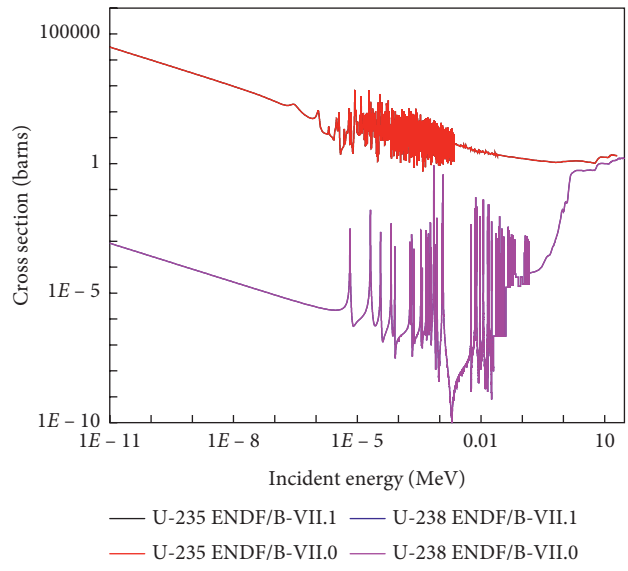

Figure 9: ^{235}U and ^{238}U fission cross sections of ENDF/B-VII.0 and ENDF/B-VII.1.

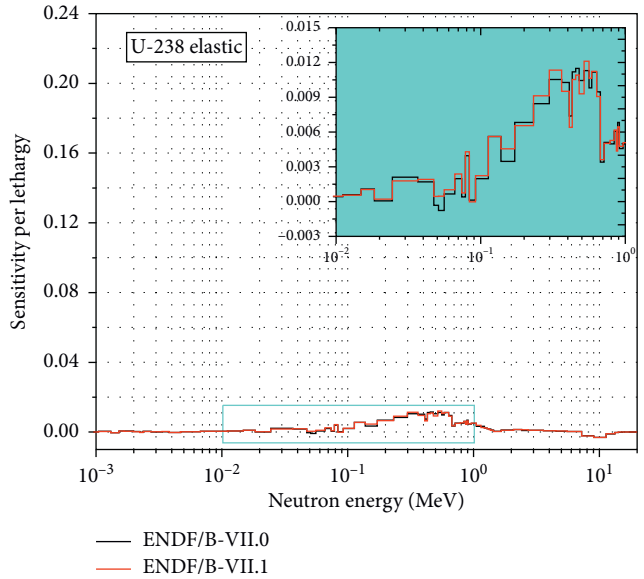

Figure 10: Energy-dependent sensitivities of k_{eff} to ^{238}U elastic scattering cross section.

the top five contributors are the (n, fission) and total ν of ^{235}U, and total ν, (n, fission) and elastic scattering of ^{238}U. The sensitivity coefficients of an isotope for a reaction strongly depend on the neutron spectrum of the system and the cross section of the isotope itself. As shown in Figure 4, the neutron spectra of the B&BR obtained by using two libraries are hard spectrum with the biggest neutron fluxes at the region from hundreds of keV to several MeV. This explains why the significant sensitivity coefficients are observed at that energy range. In detail, the sensitivity coefficients of ^{235}U total ν and fission cross section have a broad peak from the several hundreds of keV to MeV range (Figures 5 and 6), while those of ^{238}U have a sharper peak at harder energy region—several MeV (Figures 7 and 8). The sensitivity coefficients of ^{238}U total ν and fission cross section have a peak at MeV region which can be explained by its largest cross section value at several MeV. This is different from the sensitivity profile of ^{235}U total ν and fission with their peaks located at the softer energy range due to their decreasing cross sections versus the increasing of incident neutron energy (Figure 9). The sensitivities of elastic scattering of ^{238}U (Figure 10), ^{56}Fe (Figure 11), ^{23}Na (Figure 12), ^{208}Pb (Figure 13), and ^{239}Pu (Figure 14) are the most significant at energy range from 100 keV to 1 MeV since those isotopes have larger elastic scattering cross section at that energy range than that at several MeV as shown in Figure 15.

For the negative sensitivity coefficients, the capture and inelastic scattering reactions of $^{235, 238}$U and ^{56}Fe isotopes are

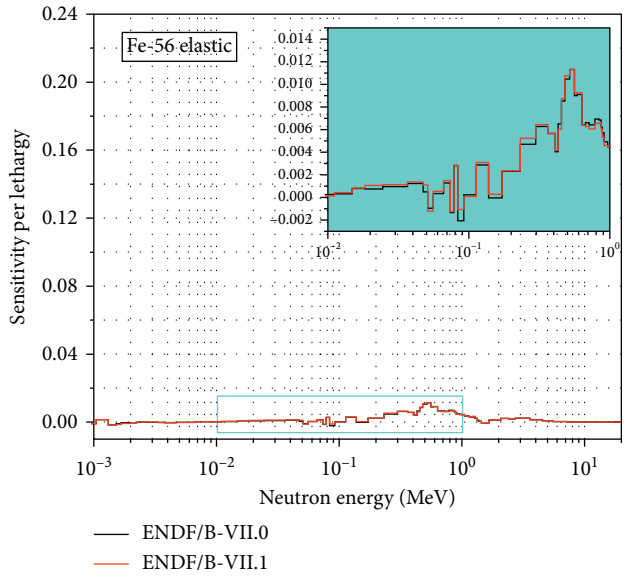

Figure 11: Energy-dependent sensitivities of k_{eff} to ^{56}Fe elastic scattering cross section.

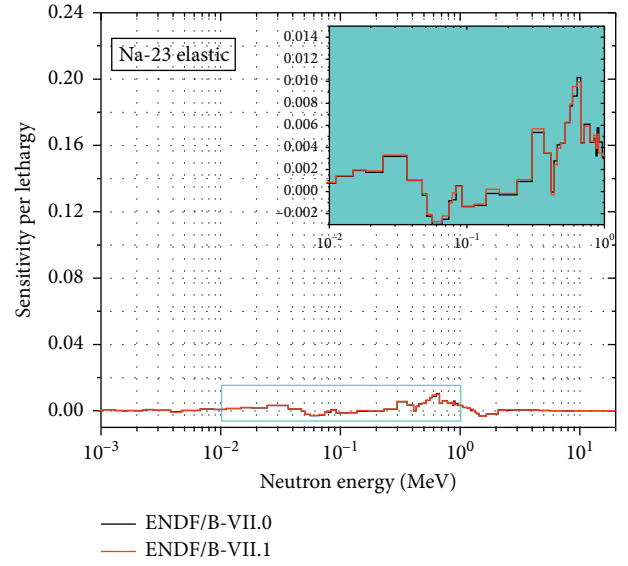

Figure 12: Energy-dependent sensitivities of k_{eff} to ^{23}Na elastic scattering cross section.

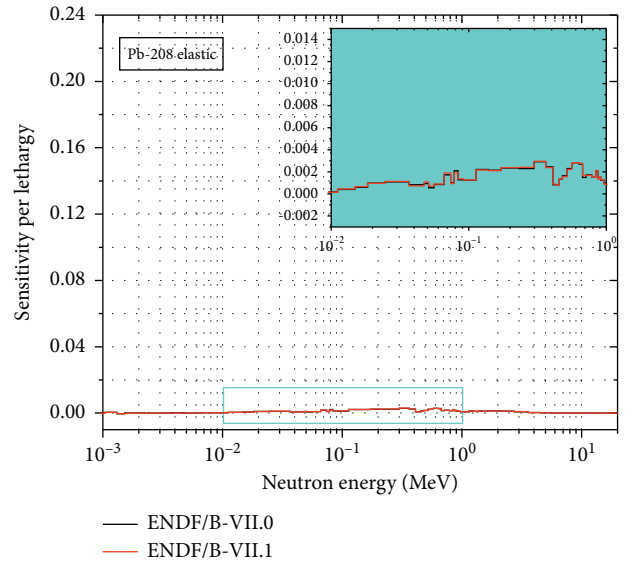

Figure 13: Energy-dependent sensitivities of k_{eff} to ^{208}Pb elastic scattering cross section.

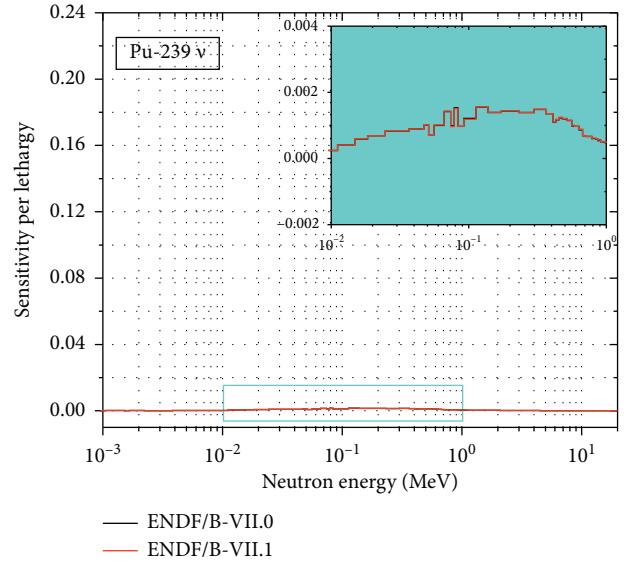

Figure 14: Energy-dependent sensitivities of k_{eff} to ^{239}Pu total ν cross section.

mainly involved. As illustrated in Figure 16, the sensitivity coefficient of the ^{238}U capture cross section has a relatively large peak at several hundreds of keV while the peak of sensitivity coefficient of ^{235}U is sharper in the same energy range (Figures 17). Figure 18 shows that the sensitivity coefficient of ^{56}Fe capture cross section mainly concentrates at the energy region from tens of keV to 1 MeV. The sensitivity coefficient of inelastic scattering cross section of ^{235,238}U and ^{56}Fe (Figures 19–21) has a peak at a very high energy range (about 2–3 MeV) since their cross sections are observed to have the peak at this region as illustrated in Figure 22.

As shown in the zoom-in region in Figure 4, the noticeable difference of neutron spectrum between the two nuclear libraries can be observed at several keV and hundreds of keV regions. Thus, we can observe the small discrepancies in the energy-dependent sensitivity profile of ENDF/B-VII.0 and ENDF/B-VII.1 at those energy regions. The inconsistency in sensitivity coefficients between two nuclear data libraries is more evident for the reactions whose cross sections have the resonance region at the above-mentioned energy ranges (illustrated in the zoom-in region in energy-dependent sensitivity profile figures).

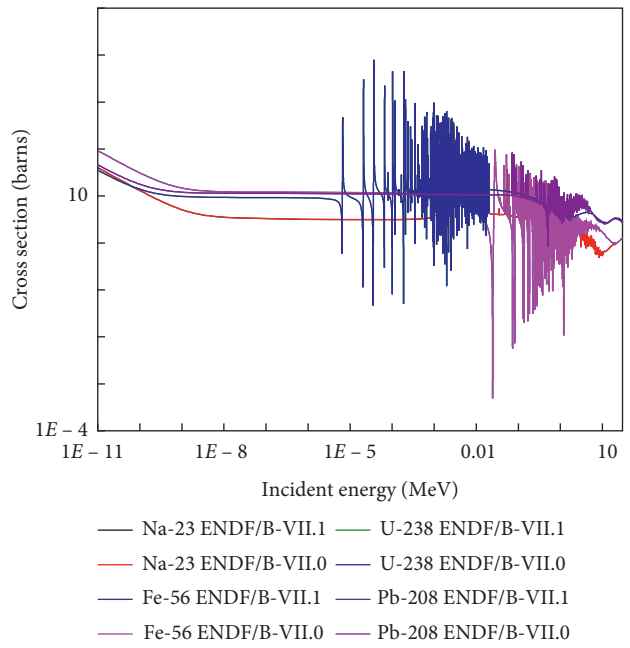

FIGURE 15: ^{23}Na, ^{56}Fe, ^{208}Pb, and ^{238}U elastic scattering cross sections of ENDF/B-VII.0 and ENDF/B-VII.1.

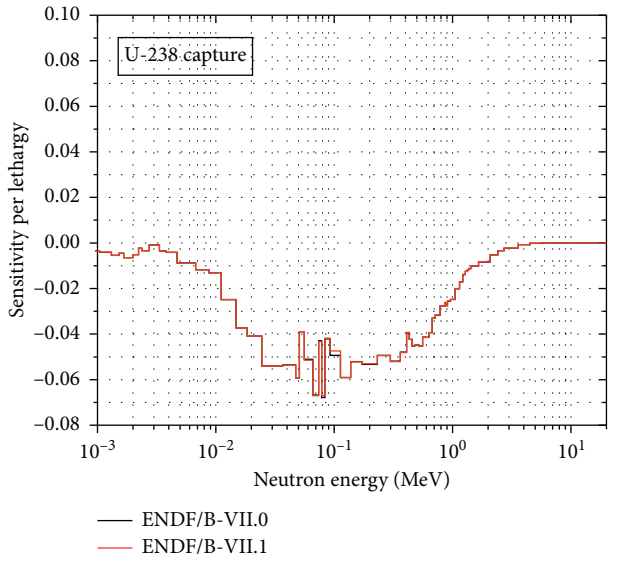

FIGURE 16: Energy-dependent sensitivities of k_{eff} to ^{238}U capture cross section.

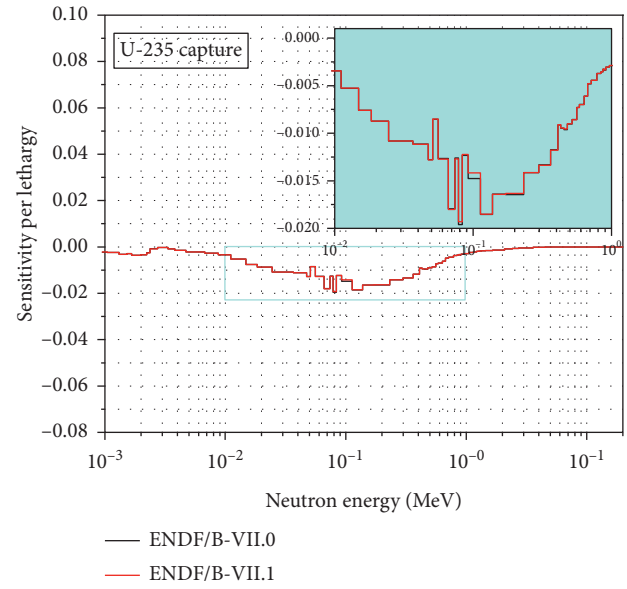

FIGURE 17: Energy-dependent sensitivities of k_{eff} to ^{235}U capture cross section.

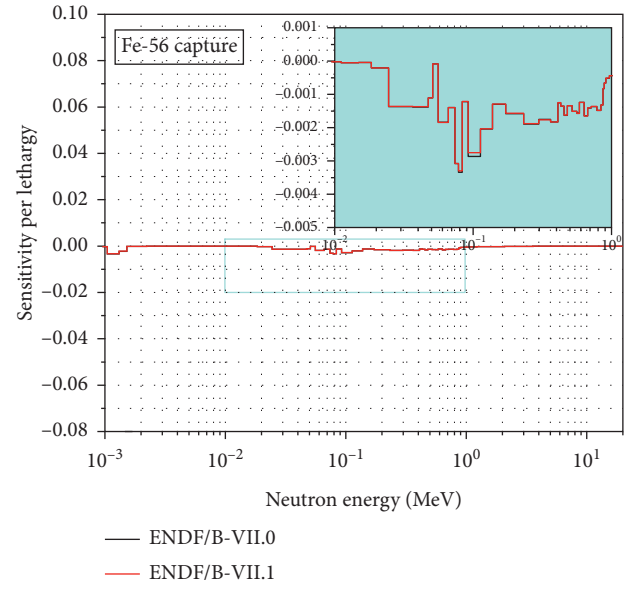

FIGURE 18: Energy-dependent sensitivities of k_{eff} to ^{56}Fe capture cross section.

4.2. Uncertainty Analysis. The uncertainty of k_{eff} for B&BR obtained by the TSUNAMI-3D module utilizing the above-mentioned 44-group and 56-group structure sensitivity is presented in Table 4. As shown in Table 4, the cross sections of ENDF/B-VII.0 and ENDF/B-VII.1 cause quite considerable uncertainty of the k_{eff} calculated result. It is about 2,084 pcm for ENDF/B-VII.0 and 2,145 pcm for ENDF/B-VII.1. As listed in Table 5, the main contribution of the k_{eff} uncertainty comes from the nuclear cross section data of ^{235,238}U and ^{56}Fe. The results reveal that the isotopes with the most significant sensitivity are also the biggest contributors to k_{eff} uncertainty. Although the sensitivity profiles of ^{235}U total ν and ^{56}Fe capture reaction between ENDF/B-VII.0 and ENDF/B-VII.1 are similar, the uncertainty due to these cross sections shows a difference between the two nuclear data libraries due to the disparity in the covariance data of these cross sections between the two nuclear data libraries, as illustrated in Figures 23 and 24.

Further investigation of the impact of nuclear data on the reactivity calculation results of the fast system was done and the CVR (when all the sodium in the system was replaced by void) and the FTC and their uncertainties were estimated.

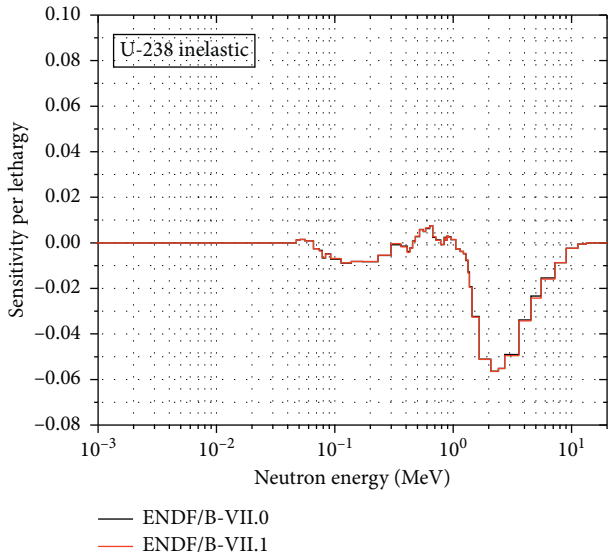

Figure 19: Energy-dependent sensitivities of k_{eff} to ^{238}U inelastic scattering cross section.

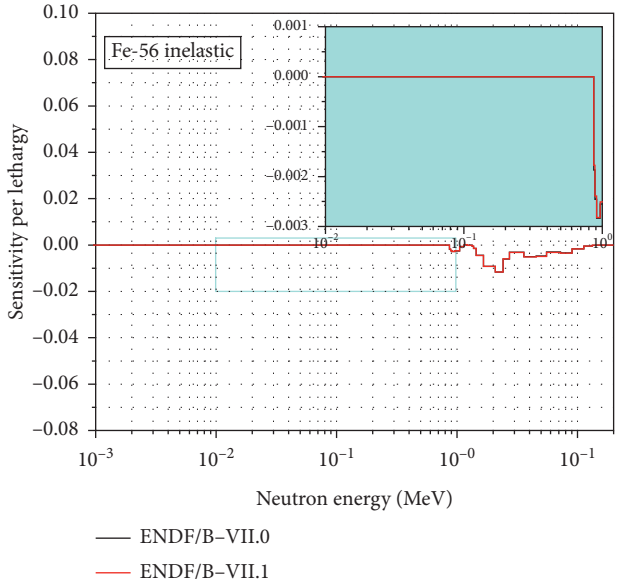

Figure 20: Energy-dependent sensitivities of k_{eff} to ^{56}Fe inelastic scattering cross section.

Since the FTC value of the fast system is small, it is important to reassure that the calculation result is reliable to discuss the safety features of the system. Regarding the CVR value of the B&BR, it is worthy to notice that the CVR in this investigation is largely negative since the voiding is performed for all regions at BOL condition in which the active core height is still relatively short. Therefore, higher neutron leakage is expected during voiding. The uncertainty can be achieved automatically using the TSAR module in SCALE6.2. The perturbed sensitivity due to coolant density or fuel temperature change was produced to obtain the uncertainty of CVR and FTC. The uncertainty of the CVR result is about 18% of reactivity which is equivalent to about 208.4 pcm and 214.7 pcm for ENDF/B-VII.0 and ENDF/B-VII.1 data libraries, respectively. The top five contributions were the elastic scattering of ^{238}U, capture of ^{235}U and ^{238}U, and elastic scattering of ^{23}Na and ^{56}Fe. For FTC results, the uncertainty is about 15% for both libraries, and the most significant contributions were found from the elastic scattering of ^{238}U and ^{56}Fe, capture of ^{235}U, and elastic scattering of ^{94}Zr and ^{57}Fe. From the S/U analyses for two library versions, the significant uncertainty of reactivity calculation

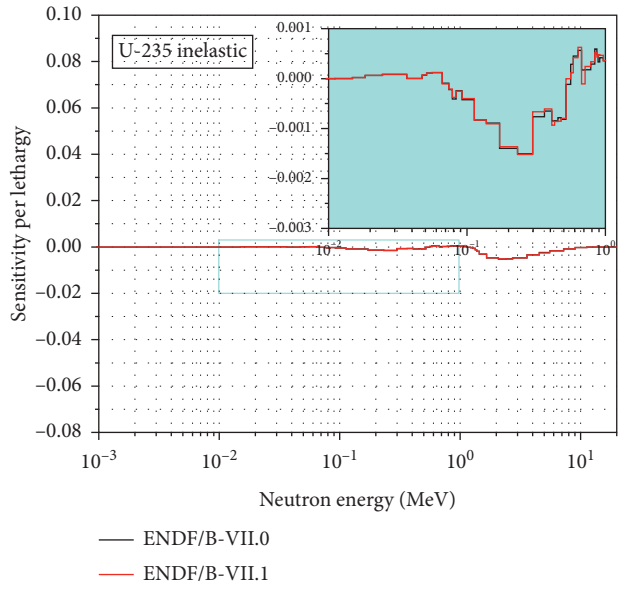

Figure 21: Energy-dependent sensitivities of k_{eff} to ^{235}U inelastic scattering cross section.

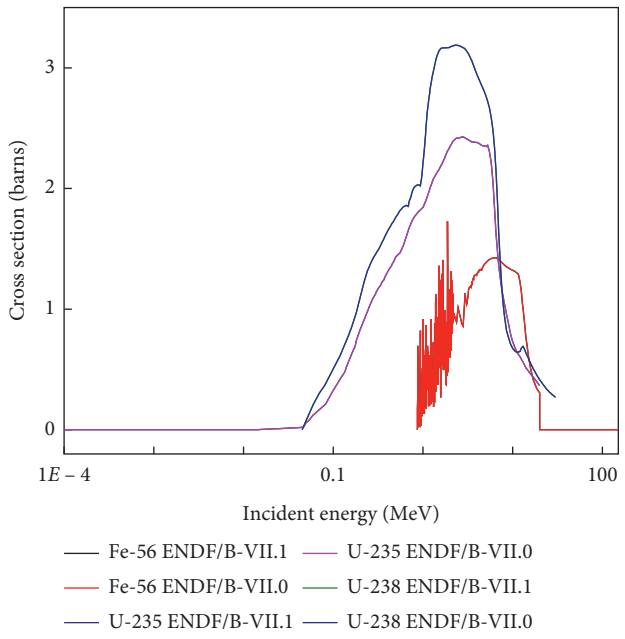

Figure 22: ^{56}Fe, ^{235}U, and ^{238}U inelastic scattering cross sections of ENDF/B-VII.0 and ENDF/B-VII.1.

Table 4: Uncertainty results of SNF-fuelled B&BR.

Parameter	ENDF/B-VII.0		ENDF/B-VII.1	
	Value	Uncertainty	Value	Uncertainty
k_{eff}	1.00165 ± 0.00004	0.020912 ± 0.000004	1.00065 ± 0.00004	0.021693 ± 0.000004
CVR (pcm)	-1151.6 ± 5.9	208.4 ± 0.7	-1191.3 ± 5.7	214.7 ± 0.8
FTC, pcm/K	-0.421 ± 0.007	0.0310 ± 0.0007	-0.410 ± 0.006	0.0310 ± 0.0009

Table 5: Top 10 contributors to k_{eff} uncertainty.

Isotopes	Nuclear data	Uncertainty for ENDF/B-VII.0	Uncertainty for ENDF/B-VII.1
^{235}U	σ_c, σ_c	$1.60E+00$	$1.62E+00$
	ν, ν	$1.23E-01$	$8.40E-02$
	σ_f, σ_f	$2.17E-01$	$2.38E-01$
^{238}U	σ_{ine}, σ_{ine}	$1.18E+00$	$1.20E+00$
	σ_c, σ_c	$2.99E-01$	$2.72E-01$
	σ_{el}, σ_{ine}	$2.92E-01$	$2.71E-01$
	ν, ν	$2.17E-01$	$2.20E-01$
	σ_{el}, σ_{el}	$5.57E-02$	$5.44E-02$
	σ_f, σ_f	$5.87E-02$	$5.87E-02$
^{56}Fe	σ_c, σ_c	$6.45E-02$	$8.81E-02$

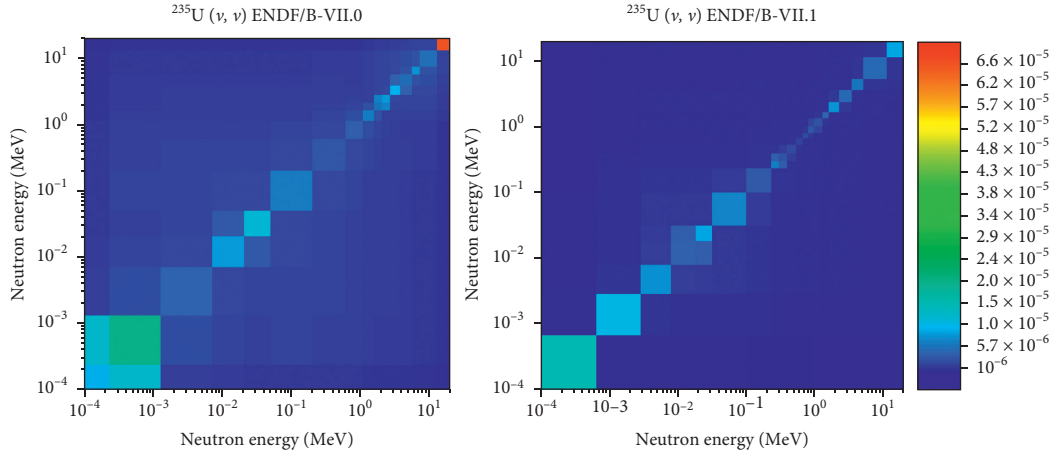

Figure 23: ^{235}U (ν, ν) 44-g and 55-g covariance matrices.

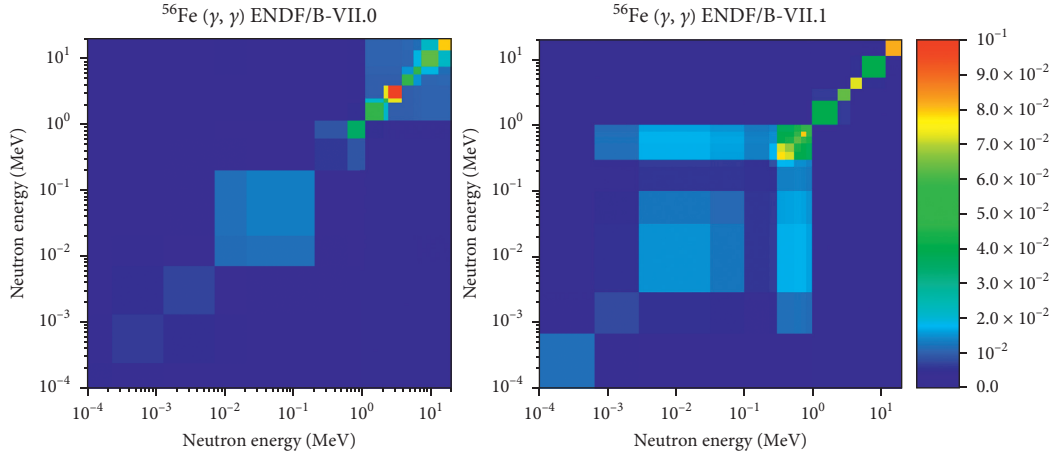

Figure 24: ^{56}Fe (capture, capture) 44-g and 55-g covariance matrices.

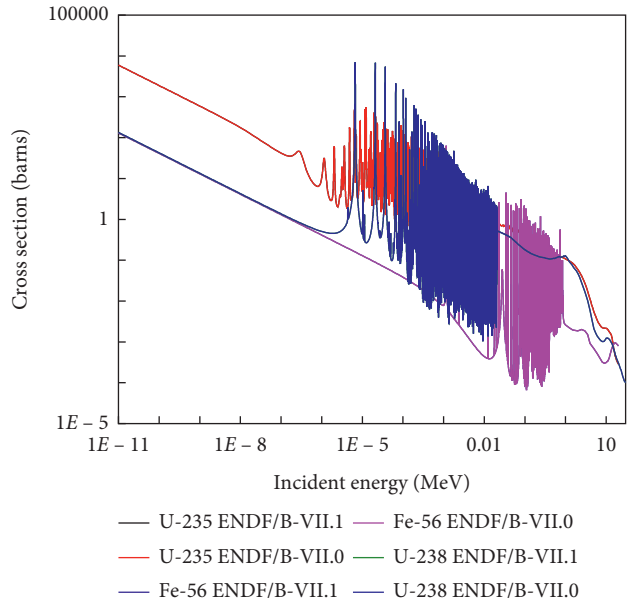

Figure 25: ^{56}Fe, ^{235}U, and ^{238}U capture cross sections of ENDF/B-VII.0 and ENDF/B-VII.1.

results should be noticed when using ENDF/B-VII.0 and ENDF/B-VII.1 libraries in fast reactors' calculation as shown in Figure 25.

5. Summary and Conclusions

The sensitivity and uncertainty analyses were conducted on the small linear B&BR by SCALE6.2 code using ENDF/B-VII.0 and ENDF/B-VII.1 nuclear data libraries. The results reveal that the uncertainty of reactivity calculation result of B&BR caused by the inaccuracy of the two libraries is significant (more than 2000 pcm), mainly from the uncertainty of $^{235,\ 238}$U and ^{56}Fe cross section data. The energy-dependent sensitivity coefficients obtained for two nuclear data libraries show that they are significant at the fast energy range. Differences in the sensitivity coefficients of the two library versions were found to be not significant. That is caused by the change of the neutron spectrum of the core, and the most significant discrepancy between the two libraries is at the energy region from several keV to 1 MeV. The uncertainty results of CVR and FTC obtained by SCALE6.2 show that the uncertainty of CVR is about 18%, and the one of FTC is about 15% of core reactivity. The top five contributors to the uncertainty of CVR accounted for the cross section errors of elastic scattering of ^{238}U, capture of ^{235}U and ^{238}U, and elastic scattering of ^{23}Na and ^{56}Fe, and those of the uncertainty of FTC were accounted for elastic scattering of ^{238}U and ^{56}Fe, capture of ^{235}U, and elastic scattering of ^{94}Zr and ^{57}Fe. The energy-dependent sensitivity coefficient is informative about the accuracy of the nuclear data at a specific energy range. From the findings of this work, it is highly recommended to improve the accuracy of the above-mentioned isotopes' cross sections at the high energy range to provide a more reliable reactivity calculation for the fast system. For future work, the uncertainty will be investigated at the end of life condition using the latest nuclear data ENDF/B-VIII.0. Moreover, the uncertainty study of the fissile isotopes conversion ratio in the B&BR is also suggested.

Data Availability

The research data cannot be shared due to privacy restrictions and can only be made available upon request to the corresponding author.

Conflicts of Interest

The authors declare that they have no conflicts of interest.

Acknowledgments

This research was funded by the Vietnam National Foundation for Science and Technology Development (NAFOSTED) under Grant no. 103.04–2019.14. D. Hartanto was supported by the Office of Vice-Chancellor for Research and Graduate Studies, University of Sharjah, UAE, under Grant no. 1802040796-P.

References

[1] D. Hartanto and Y. Kim, "Alternative reflectors for a compact sodium-cooled breed-and-burn fast reactor," *Annals of Nuclear Energy*, vol. 76, pp. 113–124, 2015.

[2] D. Hartanto, W. Heo, C. Kim, and Y. Kim, "Impacts of burnup-dependent swelling of metallic fuel on the performance of a compact breed-and-burn fast reactor," *Nuclear Engineering and Technology*, vol. 48, no. 2, pp. 351–359, 2016.

[3] D. Hartanto, C. Kim, and Y. Kim, "An optimization study on the excess reactivity in a linear breed-and-burn fast reactor (B&BR)," *Annals of Nuclear Energy*, vol. 94, pp. 62–71, 2016.

[4] C. Kim, D. Hartanto, and Y. Kim, "Neutronics feasibility of simple and dry recycling technologies for a self-sustainable

breed-and-burn fast reactor," *Annals of Nuclear Energy*, vol. 110, pp. 847–855, 2017.

[5] D. Hartanto, *A design and physics study of a compact sodium-cooled breed-and-burn fast reactor*, Ph.D. Dissertation, KAIST, Daejeon, South Korea, 2015.

[6] T. M. Vu and T. Kitada, "Impact of thorium capture cross section uncertainty on the thorium utilized ads reactivity calculation," *Science and Technology of Nuclear Installations*, vol. 2014, Article ID 509858, 4 pages, 2014.

[7] F. Osuský, Š. Čerba, J. Lüley, B. Vrban, J. Haščík, and V. Nečas, "On gas-cooled fast reactor designs - nuclear data processing with sensitivity, uncertainty and similarity analyses," *Progress in Nuclear Energy*, vol. 128, Article ID 103450, 2020.

[8] E. Fridman, V. Valtavirta, and M. Aufiero, "Nuclear data sensitivity and uncertainty analysis of critical VENUS-F cores with the Serpent Monte Carlo code," *Annals of Nuclear Energy*, vol. 138, Article ID 107196, 2020.

[9] M. B. Chadwick, P. Obložinský, M. Herman et al., "ENDF/B-VII.0: next generation evaluated nuclear data library for nuclear science and technology," *Nuclear Data Sheets*, vol. 107, no. 12, pp. 2931–3060, 2006.

[10] M. B. Chadwick, M. Herman, P. Obložinský et al., "ENDF/B-VII.1 nuclear data for science and technology: cross sections, covariances, fission product yields and decay data," *Nuclear Data Sheets*, vol. 112, no. 12, pp. 2887–2996, 2011.

[11] B. Rearden and M. Jesse, Eds., *SCALE Code System, ORNL/TM-2005/39*, Oak Ridge National Laboratory, Oak Ridge, TN, United States, Version 6.2.3, 2018.

[12] C. Kim, D. Hartanto, and Y. Kim, "Uranium enrichment reduction in the prototype gen-IV sodium-cooled fast reactor (PGSFR) with PbO reflector," *Nuclear Engineering and Technology*, vol. 48, no. 2, pp. 351–359, 2016.

[13] B. T. Rearden, M. L. Williams, M. A. Jessee, D. E. Mueller, and D. A. Wiarda, "Sensitivity and uncertainty analysis capabilities and data in SCALE," *Nuclear Technology*, vol. 174, no. 2, pp. 236–288, 2011.

[14] A. Hara, T. Takeda, and Y. Kikuchi, "SAGEP: two-dimensional sensitivity analysis code based on generalized perturbation theory," *Tech. Rep. JAERI-M*, vol. 84-027, pp. 1–30, 1984.